Journal of Anatomy

J. Anat. (2012) **221**, pp417–426 doi: 10.1111/j.1469-7580.2012.01562.x

The inner ear of *Diacodexis*, the oldest artiodactyl mammal

M. J. Orliac,[1,2] J. Benoit[1] and M. A. O'Leary[2]

[1]*ISE-M, Université Montpellier2, Montpellier, France*
[2]*Department of Anatomical Sciences, Stony Brook University, Stony Brook, NY, USA*

Abstract

We provide the first detailed description of the inner ear of the oldest artiodactyl, *Diacodexis*, based on a three-dimensional reconstruction extracted from computed tomography imagery of a skull of *Diacodexis ilicis* of earliest Wasatchian age (ca. 55 Ma). This description provides new anatomical data for the earliest artiodactyls, and reveals that the bony labyrinth of *Diacodexis* differs greatly from that of modern artiodactyls described so far. The bony labyrinth of *Diacodexis* presents a weakly coiled cochlea (720 °), a secondary common crus, a dorsal extension of the anterior semicircular canal more pronounced than that of the posterior one, and a small angle between the basal turn of the bony cochlear canal and the lateral semicircular canal. This suite of characters also occurs in basal eutherian mammals. *Diacodexis* strongly resembles small living tragulid ruminants in its overall body shape and hindlimb proportions. Comparison of the bony labyrinth of *Diacodexis* to that of the tragulid *Moschiola meminna* (Indian mouse deer) reveals great morphological difference in cochlear shape and semicircular canal disposition. The shape of the cochlea suggests that *Diacodexis* was a high-frequency hearing specialist, with a high low-frequency hearing limit (543 Hz at 60 dB). By comparison, the estimated low-frequency limit of *Moschiola meminna* is much lower (186.0 Hz at 60 dB). We also assess the locomotor agility of *Diacodexis* based on measurements of the semicircular canals. Locomotor agility estimates for *Diacodexis* range between 3.62 and 3.93, and suggest a degree of agility compatible with a nimble, fast running to jumping animal. These results are congruent with the postcranial functional analysis for this extinct taxon.

Key words: Artiodactyla; bony labyrinth; computed tomography; Eocene; *Moschiola*; Tragulidae.

Introduction

The hoofed mammal clade Artiodactyla appears in the fossil record at the very base of the Eocene (≈55.8 million years ago) with *Diacodexis* Cope, 1882, a squirrel-sized, deer-like small artiodactyl (Rose, 2006). Species of *Diacodexis* have been reported from Eocene fossil localities on all continents of the Northern hemisphere (e.g. Guthrie, 1971; Godinot, 1981; Sudre et al. 1983; Thewissen et al. 1983; Kumar & Jolly, 1986; Gingerich, 1989; Smith et al. 1996; Bajpai et al. 2005; Kumar et al. 2010), and the dental, cranial and postcranial features of the genus are now well known. Skeletons of *D. metsiacus* (Rose, 1982, 2006) and *D. pakistanensis* (Thewissen & Hussain, 1990) have been interpreted to be those of a fast running to jumping mammal (Rose, 1982, 2006). *Diacodexis* species had larger and longer hindlimbs relative to forelimbs, as well as a long tail for counterbalance (Rose, 1982). The crural index for *Diacodexis* falls in the range of indices observed in modern ruminants and rabbits (Rose, 1982). In sum, *Diacodexis* may have employed a combination of both cursorial and saltatorial habits. Even though the small size of *Diacodexis* has no equivalent in modern artiodactyls, the resemblance of this species to modern tragulid ruminants in limb proportions and locomotory habits has led scientists to regard tragulids as the closest living analog of *Diacodexis* (Rose, 1982, 2006).

Descriptions and illustrations of the inner ears of any artiodactyls are scarce. Except for the seminal work of Gray (1907), such descriptions are restricted to Suidae (Lovel & Harper, 2007; Ekdale, 2009), Cetacea (Spoor et al. 2002; Bajpai et al. 2009; Thewissen et al. 2009) and the extinct Merycoidodontidae (Ekdale, 2009). The inner ear contains detailed anatomical features that can be integrated into phylogenetic studies (e.g. Luo & Gingerich, 1999; Ekdale et al. 2004; Lebrun et al. 2010; Benoit et al. in press), but such information has not yet been used extensively in artiodactyl phylogenetics. In this study, we use high-resolution x-ray computed tomography to investigate the inner ear of

Correspondence
Maureen A. O'Leary, Department of Anatomical Sciences, HSC-T-8 (040), Stony Brook University, Stony Brook, NY 11794-8081, USA.
E: maeva.orliac@univ-montp2.fr

Accepted for publication *7 August 2012*
Article published online *2 September 2012*

the North American Diacodexeidae *Diacodexis ilicis* of earliest Wasatchian age (Sand Coulee beds, Clark Fork basin, ≈55 million years ago; Gingerich, 1989).

The inner ear is composed of two primary functional parts: the cochlea, which is the organ of hearing; and the vestibular system (comprising the vestibule and semicircular ducts), involved in coordinating posture and body movements during locomotion (Silcox et al. 2009). As such, inner ear morphology has been examined for its correlation with hearing (e.g. West, 1985; Ketten et al. 1992; Manoussaki et al. 2008; Coleman & Colbert, 2010; Coleman et al. 2010) and locomotor behavior in mammals (e.g. Spoor et al. 2002; Yang & Hullar, 2007; Silcox et al. 2009). In order to investigate the morphological similarities and differences between the earliest artiodactyl and its modern tragulid ecological and anatomical analog, we compare the inner ear of *Diacodexis* to that of the Indian mouse deer, *Moschiola meminna* (Erxleben, 1777), one of the smallest living tragulid species (Mendoza et al. 2006). We ask here if the living tragulid *M. meminna* and *Diacodexis*, which have similar limb proportions, also share a similar locomotor agility signal in the semicircular canals. We describe the labyrinth morphology of these species and discuss the hypothetical ancestral labyrinth morphology previously proposed for that Artiodactyla (Ekdale, 2009).

Materials and methods

Specimens

We reconstructed the labyrinth endocast of the left *in-situ* petrosal of the cranium of AMNH VP 16141 (American Museum of Natural History, New York, USA). A detailed description of the basicranium of this specimen was previously published by Coombs & Coombs (1982) who referred it to *Diacodexis* sp. The cranium was collected during an AMNH expedition in 1912, and the locality is listed as '3 miles South East, mouth of Pat O'Hara Creek, Clark's Fork Basin, Wyoming' in the Sand Coulee beds of the Willwood formation. The Sand Coulee beds yield a fauna of earliest Wasatchian in age (about 55 million years ago; Gingerich, 1989), which corresponds to one of the earliest occurrences of *Diacodexis*. *Diacodexis ilicis* Gingerich, 1989 has been reported from this locality (Gingerich, 1989; Rose et al. 2012). Unfortunately, the distinctive characters of *D. ilicis* are mainly found in the lower dentition (Rose et al. 2012), and no mandible is associated with the cranium of AMNH VP 16141. The size of the upper teeth of AMNH VP 16141, however, falls within the range of variation of those of *D. ilicis* (Rose et al. 2012), and even if the teeth in AMNH VP 16141 are slightly worn, their shape and general features are congruent with the morphology of specimens of *D. ilicis* (Rose et al. 2012: fig. 51). The position of the petrosals in the cranium is assumed to be unaffected by the post mortem dorsoventral deformations that mainly deformed the roof of the cranium. The precise orientation of the petrosal in the cranial cavity and the orientation of the inner ear were determined after *in-situ* translucent rendering of the skull, and of the petrosal (Fig. 1), respectively.

We describe the petrosal of Tragulidae using the exemplar taxon *M. meminna* based on a left *in-situ* petrosal bone (UM2 58V). We also compare the fossil with the living suid *Sus scrofa* to establish a slightly broader basis of comparison. Comparison with *S. scrofa* is based on the computed tomography (CT) scan of a left *in-situ* petrosal bone (UM2 not numbered), and on the description provided by Ekdale (2009).

CT scanning and digital endocast extraction

The skull of *D. ilicis* was scanned in its entirety in the coronal plane using the high-resolution GE phoenix|vtome|x s240 industrial CT scanner at the American Museum of Natural History (New York). The scans resulted in 1751 slices with dimensions of 994 × 994 pixels. The slices have a 34.39 μm thickness and are spaced 34.39 μm apart. We scanned the ear region of the skull of *M. meminna* with the Skyscan/1076/invivo CT scanner at the Institut des Sciences de l'Evolution, Montpellier, Université Montpellier2 (France). The scans resulted in 630 slices with dimensions of 1140 × 1144 pixels. The slices have a 71.66 μm thickness and are spaced 71.66 μm apart. Two-dimensional slices are reconstructed from X-rays using Vgstudiomax® (version 1.2; VolumeGraphics GmbH, 2004).

We extracted the digital endocast using the segmentation tools of AVIZO 6.3 (Visualization Sciences Group) and calculated volumes by surface integration. We segmented the cochlea in a separate labelfield module to estimate its volume separately.

Measurements

We made linear measurements from the inner ear model using the 3D measurement tool of AVIZO. Measurements taken follow the protocol illustrated by Ekdale (2009). Semicircular canal length could be measured from the point of the canal farthest away from the vestibule and semicircular canal width perpendicular to this line, at the widest expanse of the canal arc. We made measurements from the center of each canal following Spoor et al. (2007). We calculated the radius of curvature of each canal using the equation of Spoor & Zonneveld (1998) [(0.5 ($l + w$)/2), where l = length and w = width of canal]. The number of turns was measured according to the protocol of West (1985).

Predicting locomotor agility and hearing abilities

Locomotor agility

Based on the agility scores assigned to a sample of 210 extant mammals by Spoor et al. (2007), Silcox et al. (2009) determined

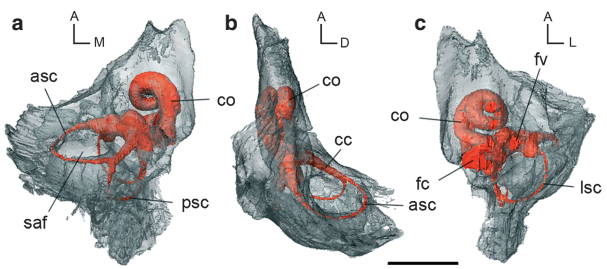

Fig. 1 *In-situ* 3D reconstruction from CT data of the bony labyrinth of the left petrosal of *Diacodexis ilicis* (AMNH VP 16141) in (a) dorsomedial, (b) lateral and (c) ventrolateral views. Scale bar: 1 cm. asc, anterior semicircular canal; cc, common crus; co, cochlear canal; fc, fenestra cochleae; fv, fenestra vestibuli; lsc, lateral semicircular canal; psc, posterior semicircular canal; saf, subarcuate fossa; orientations: A, anterior; D, dorsal; L, lateral; M, medial.

equations to predict locomotor agility in extinct mammals using the radii of the three semicircular canals. We used equations from Silcox et al. (2009) to predict the locomotor agility for *D. ilicis* and compare it with *M. meminna* and with the extant artiodactyls sampled by Silcox et al. (2009). These equations are: (AGIL = agility; ASCR = anterior semicircular canal radius; BM = body mass in grams; LSCR = lateral semicircular canal radius; PSCR = posterior semicircular canal radius; SCR = average semicircular canal radius):

$$\text{ASCR: } \log_{10}\text{AGIL} = 0.850 - 0.153\ (\log_{10}\text{BM}) + (0.706\ (\log_{10}\text{ASCR}))$$
$$\text{PSCR: } \log_{10}\text{AGIL} = 0.881 - 0.151\ (\log_{10}\text{BM}) + (0.677\ (\log_{10}\text{PSCR}))$$
$$\text{LSCR: } \log_{10}\text{AGIL} = 0.959 - 0.1670\ (\log_{10}\text{BM}) + (0.854\ (\log_{10}\text{LSCR}))$$
$$\text{SCR: } \log_{10}\text{AGIL} = 0.948 - 0.188\ (\log_{10}\text{BM}) + (0.962\ (\log_{10}\text{SCR}))$$

Body mass estimates for *D. ilicis* are based on dental, cranial and postcranial measurements. Body mass estimates based on dental measurements were derived from the regressions of Damuth (1990) for non-selenodont ungulates calculated from the first lower molar length: $[(\log_{10}\text{BM}) = 3.17\ \log_{10}\ (\text{m1 length}) + 1.04]$. Body mass estimates based on cranial measurements were derived from Janis (1990) regression for all ungulates based on estimates of total skull length $[(\log_{10}\text{BM}) = 2.975\ \log_{10}\ (\text{total skull length}) - 2.344]$. Body mass estimates based on postcranial measurements were derived from the equation of Martinez & Sudre (1995) based on astragalus measurements $[\text{BM} = 3.16\ (\text{length astragalus} \times \text{width astragalus})^{1.482}]$. Body mass estimates of *D. ilicis* range from 554 g (postcranial measurements) up to 935 g (skull length). For further details on body mass estimates calculation, see Orliac & Gilissen (2012, ESM) .

The range of locomotor agility predictions for *D. ilicis* based on these equations is given in Table 1.

Hearing abilities

As noted above, Manoussaki et al. (2008) demonstrated that the radii ratio of the cochlea (quotient of the radius of the basal turn and the radius of the apical turn of the cochlea) was linearly correlated with the log of low-frequency hearing abilities limit for a sample of marine and land mammal species. We use the equation of Manoussaki et al. (2008) to predict *D. ilicis* low-frequency hearing limit (f = low-frequency hearing limit; p = radii ratio = R_{base}/R_{apex}): $f = 1.507\ \exp[-0.578\ (p - 1)]$. We measured the radii of curvature (R_{base} and R_{apex}) following the procedure of Manoussaki et al. (2008).

Table 1 Body mass estimates and locomotor agility scores for the 3D reconstructions from CT data of labyrinth endocasts of *Diacodexis ilicis* and *Moschiola meminna*. Body mass estimates (BM) for *Diacodexis* are derived from estimates based on: a, astragalus measurements; b, skull length; and c, length of the first lower molar.

	BM (g)	ASCR	LSCR	PSCR	SCR
Diacodexis ilicis	554 (a)	3.93	3.81	3.62	3.84
	935 (b)	3.63	3.49	3.35	3.48
	737 (c)	3.77	3.63	3.47	3.64
Moschiola meminna	4000	3.29	3.60	3.42	3.46
Sus scrofa	55 000	2.54	2.43	2.65	2.43
Gazella bennetti	23 000	3.31	3.20	3.35	3.40
Oryctolagus cuniculus	1740	3.70	3.80	3.50	3.80

Values from Silcox et al. (2009) are provided for *Sus scrofa*, *Gazella bennetti* and *Oryctolagus cuniculus* for comparison.
ASCR, anterior semicircular canal radius agility score; BM, body mass; LSCR, lateral semicircular canal radius agility score; PSCR, posterior semicircular canal radius agility score; SCR, average semicircular canal radius agility score.

Comparative description

The bony labyrinth of *D. ilicis* largely fills the petrosal volume (Fig. 1). The cochlea occupies half of the volume of the pars cochlearis and represents almost the entire thickness of this part of the petrosal (Fig. 1b). The semicircular canals are spread widely through the mastoid region of the pars canalicularis, which does not extend much beyond the common crus height dorsomedially (Fig. 1b). The anterior semicircular canal (ASC) borders the wide and deep subarcuate fossa (Fig. 1a,b); the wide lateral semicircular canal (LSC) extends posteriorly to the edge of the petrosal (Fig. 1c). Measurements of the 3D reconstruction of the labyrinth endocasts of *D. ilicis* and *M. meminna* are provided in Table 2.

The cochlear canal

The cochlear canal is the bony structure that houses the membranous cochlea. The spiral canal of the cochlea of *D. ilicis* completes two full turns (rotation of 720 °). The second turn does not contact the basal turn and is separated

Table 2 Measurements of 3D reconstructions from CT data of bony labyrinth endocasts of the earliest Eocene dichobunoid artiodactyl *Diacodexis ilicis*, and of the living tragulid *Moschiola meminna*.

	Diacodexis ilicis	*Moschiola meminna*
Stapedial ratio	1.78	1.41
Cochlear coiling	720 °	990 °
Cochlear spiral length (mm)	7.35	19.00
Cochlear canal volume (mm^3)	6.53	20.98
Labyrinth volume (mm^3)	11.77	33.08
Cochlear canal aspect ratio	0.54	0.46
Angle lat-ant	73.00 °	89 °
Angle lat-post	81.00 °	97 °
Angle ant-post	95.00 °	84 °
ASC H–W (mm)	3.49–3.36	3.93–4.23
ASC R (mm)	1.71	2.04
ASC L (mm)	7.35	8.50
PSC H–W (mm)	2.39–3.09	3.77–4.06
PSC R (mm)	1.37	1.95
PSC L (mm)	4.55	8.15
LSC H–W (mm)	2.17–2.79	3.43–3.44
LSC R (mm)	1.24	1.71
LSC L (mm)	7.00	8.15

ASC, anterior semicircular canal; LSC, lateral semicircular canal; PSC, posterior semicircular canal; following a semicircular canal name: H, height; L, length; R, radius; W, width.

from the basal turn until the apex (Figs 2b and 3b). The primary and secondary osseous spiral laminae, marking the division between the scala tympani and the scala vestibuli of the cochlear canal (Meng & Fox, 1995), are visible on the digital reconstruction of the labyrinth endocast of *D. ilicis* (Fig. 2a,c), as well as on coronal CT images (Fig. 4). The secondary osseous lamina, projecting from the outer wall of the cochlear canal, is variably present or absent in mammals but is commonly present in therians (e.g. Meng & Fox, 1995; Ekdale, 2009). In *D. ilicis*, it extends from the fenestra cochleae until the medialmost part of the basal turn (first half of the basal turn of the cochlear canal, 180 °). The first turn is dorso-ventrally compressed and much wider than the second one. The cochlear spiral of *Diacodexis* is flat-

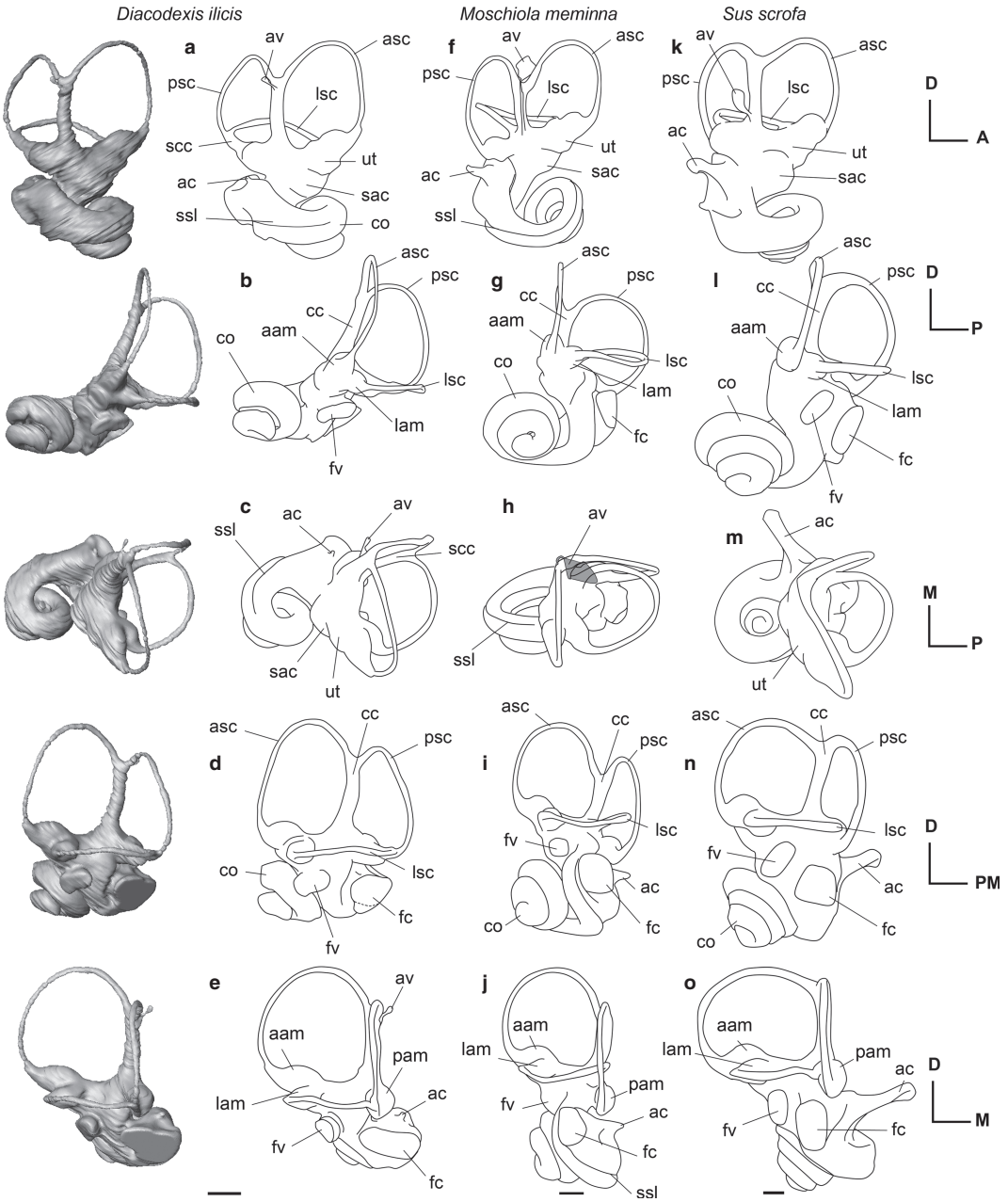

Fig. 2 3D reconstructions from CT data of the left bony labyrinth of (a–e) *Diacodexis ilicis* (AMNH VP 16141), line drawings of the left bony labyrinth of (f–j) *Moschiola meminna* (UM2 58V) and (k–o) *Sus scrofa* (UM2, not numbered) shown in anteromedial (a, f, k), lateral (b, g, l), dorsal (c, h, m), posterolateral (d, i, n), posterior (e, j, o) views. Scale bar: 5 mm. aam, anterior ampulla; ac, aqueduct cochleae; asc, anterior semicircular canal; av, aqueduct vestibuli; cc, common crus; co, cochlear canal; fc, fenestra cochleae; fv, fenestra vestibuli; lam, lateral ampulla; lsc, lateral semicircular canal; pam, posterior ampulla; psc, posterior semicircular canal; sac, saccule; scc, secondary common crus; ssl, secondary osseous spiral lamina; ut, utricule.

tened with an aspect ratio of 0.54. The fenestra cochleae (fenestra rotunda) are wide, elliptical and located at the level of the much smaller fenestra vestibuli (fenestra ovalis; Figs 1c and 2d). The cochlear aqueduct (aqueductus cochleae), housing the perilymphatic duct, emerges at the posterodorsal edge of the fenestra cochleae, and is oriented posteriorly. It is circular in cross-section and very short (0.34 mm; Fig. 2a,c).

The cochlear canals of *Diacodexis* and *Moschiola* differ markedly in their general shape and in the orientation of particular features (Fig. 2a,e vs. f–j). The spiral canal of the cochlea of *M. meminna* coils to a greater degree than that of *D. ilicis* (Fig. 3a vs. b; Table 2). The second turn of the cochlear canal of *M. meminna* overlies the basal turn and the secondary osseous lamina extends to more than half of

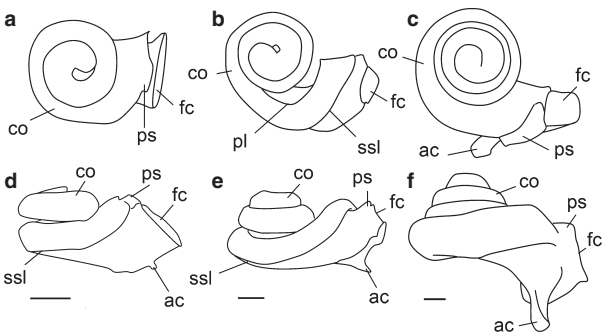

Fig. 3 Line drawings of the 3D reconstructions from CT data of the cochleae (a, d) *Diacodexis ilicis* (AMNH VP 16141), (b, e) *Moschiola meminna* (UM2 58V) and (c, f) *Sus scrofa* (UM2, not numbered) shown in apical (a–c) and medial (d–f) views. Scale bar: 5 mm. ac, aqueduct cochleae; co, cochlear canal; fc, fenestra cochleae; ssl, secondary osseous spiral lamina; pl, primary osseous spiral lamina; ps, outpocketing for perilymphatic sac.

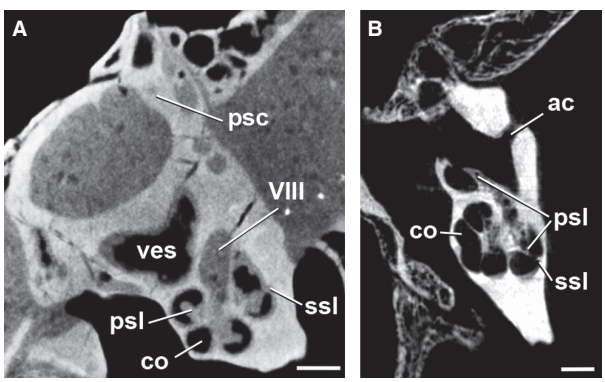

Fig. 4 Transverse CT image through the ear region of the skull of (A) *Diacodexis ilicis* (AMNH VP 16141), (B) *Moschiola meminna* (UM2 58V), showing the internal anatomy of the left petrosal. The secondary osseous spiral lamina is visible as a faint structure projecting from the meatal wall of the cochlear canal. Scale bar: 5 mm. ac, cochlear aqueduct; co, cochlear canal; psc, posterior semicircular canal; psl, primary osseous spiral lamina; ssl, secondary osseous spiral lamina; ves, vestibule; VIII, opening for vestibulocochlear nerve (Cranial Nerve VIII).

the basal turn (270 ° vs. 180 °). The cochlear spiral of *M. meminna* is flattened as in *Diacodexis* and even presents a smaller aspect ratio (0.46 vs. 0.54). The cochlear canal of *M. meminna* contributes a relatively greater amount to the total volume of the bony labyrinth (63.42% vs. 55.48%). The fenestra cochleae are situated more anteriorly and more ventrally in *M. meminna*, and have a greater ventral extension (as in *S. scrofa*; Fig. 2d vs. i). The cochlear aqueduct of *M. meminna* is longer and originates more posteriorly. The angle formed by the planes of the first turn of the cochlea and the LSC is much greater in *M. meminna* than in *Diacodexis* (42 ° vs. 13 °). The orientation of the axis of the cochlear spiral is more posterior (Fig. 2a–e vs. f–j). The labyrinth in *M. meminna* is taller dorsoventrally, due to the posteroventral inclination of the cochlea and to the weak coiling of the first part of the basal turn.

The cochlear canal of *D. ilicis* mainly differs from that of *S. scrofa* in being more weakly coiled (2 turns, 720 ° vs. 3.75 turns in *S. scrofa*, 1350 °). The length of the cochlear canal of *D. ilicis* is much shorter (7.35 mm vs. 22.89 mm), but this is partly due to the smaller size of the labyrinth in *D. ilicis*. In *S. scrofa*, the first turn overlies the second and all turns are tightly apposed (Figs 2l and 3f). According to Ekdale (2009), there is no lamina secundaria in *S. scrofa*. The aspect ratio of the cochlear spiral of *Diacodexis* is markedly smaller than that of *S. scrofa* (0.71; Ekdale, 2009), the cochlea of which has a higher profile, due to a greater coiling. Although the cochlear canal of *S. scrofa* is more voluminous (36.25 mm^3; Ekdale, 2009) than the cochlear canal of *D. ilicis* (11.77 mm^3), the structure contributes a comparable amount to the total volume of the bony labyrinth in both species (55.48% in *D. ilicis*; 58.6% in *S. scrofa*). The fenestra cochleae of *S. scrofa* are more elongated dorsoventrally with a greater ventral extension than *D. ilicis*. The cochlear aqueduct of *D. ilicis* is very short compared with that of *S. scrofa,* which consists of a long canal (0.34 mm vs. 2.64 mm) that is triangular in cross-section (Ekdale, 2009). As in *M. meminna*, the angle formed by the planes of the first turn of the cochlea and the LSC is greater in *S. scrofa* (29 °) than in *Diacodexis* (13 °). The axis of the cochlear spiral is oriented more medially in *S. scrofa* than in *D. ilicis*, which has a more vertical spiral.

The vestibule

The vestibule in the pars canalicularis (Fig. 1) is visible as the endocasts of the saccule (*recessus sphericus*) and the utricle (*recessus ellipticus*). In *Diacodexis*, both *recessi* are gently bulbous and the delineation between the structures is distinct in antero-medial view (Fig. 2a). The saccule is visible on the endocast as a bulge medial to the fenestra vestibuli (Fig. 2d). The utricle, slightly less inflated than the saccule, is visible as a swelling of the vestibule ventral to the ampulla of the ASC (Fig. 2a). The vestibular aqueduct (aqu-

eductus vestibuli), housing the endolymphatic duct, consists of a very thin canal protruding from the anterior side of the dorsalmost part of the common crus (crus commune). It extends dorsomedially until reaching the dorsalmost part of the common crus (Fig. 2a), and probably fused to the common crus space but its origin cannot be determined with precision.

The utricule and saccule are less inflated in *M. meminna*, but their separation is still distinct. As in *Diacodexis*, the vestibular aqueduct of *M. meminna* is a very thin canal, protruding from the anterior side of the dorsalmost part of the common crus and extending dorsomedially until reaching the dorsalmost part of the common crus (Fig. 2f,h). It is tightly apposed to the common crus and originates at the base of it.

The saccule of *D. ilicis* is less inflated than that of *S. scrofa* and is ellipsoid (vs. hemi-spherical for *S. scrofa*). Compared with *S. scrofa*, the fenestra vestibuli of *D. ilicis* is located in a more ventral position, at the level of the fenestra cochleae (lateral view of the lateral canal, when it is positioned horizontally; Fig. 2d vs. n). In *S. scrofa*, the vestibular aqueduct is also thin, but it originates from the vestibule, just anterior to the common crus, and extends dorsomedially until half the height of the common crus.

Semicircular canals

The ASC of *Diacodexis* has the greatest radius and length of the three semicircular canals (Table 2). Its medialmost part is bent posteriorly relative to the horizontal plane. The anterior ampulla is more inflated than the posterior one. The posterior semicircular canal (PSC) is smaller than the anterior one and its shape is more flattened. In *D. ilicis*, the posterior limb of the LSC fuses with the posterior canal to form a long and narrow secondary *crus commune* (1.15 mm; Fig. 2a,c). Inflections of its posterior and lateral surfaces delineate the profiles of the two semicircular canals and permit differentiation of the course of each canal. The angle between the ASC and LSC is the smallest, and the angle between the ASC and PSC is the greatest (Table 2). Each semicircular canal ends in an ampulla where it connects to the vestibule. The posterior ampulla is the most inflated. The posterior and lateral ampullae attach to the vestibule in the same horizontal plane, and the anterior ampulla is located slightly dorsal to the common crus.

Like in *D. ilicis*, the ASC of *M. meminna* shows the greatest dorsal extension, and is the greatest in terms of radius and length (Table 2). The taxa, however, differ by the shape of their semicircular canals. The medial edge of the PSC of *Diacodexis* is straighter, giving this canal a less circular profile. The LSC has a slight dorsal inflection in *Diacodexis*, whereas *M. meminna* shows a ventral inflection. This canal is more anteroposteriorly compressed in *M. meminna*. The secondary common crus observed in *Diacodexis* is not present in *M. meminna*, the LSC of which enters the vestibule in a much more dorsal position than the PSC, at the base of the common crus. The angulations of the semicircular canals of *M. meminna* are markedly different from those in *Diacodexis* (Table 2): the angle between the ASC and PSC is the smallest (contra ASC/LSC in *Diacodexis*), and the angle between the LSC and PSC the greatest (contra ASC/PSC in *Diacodexis*).

As in *D. ilicis* and *M. meminna*, the ASC of *S. scrofa* has the greatest radius. The angle between the ASC and LSC is the smallest one in both *D. ilicis* (76 °) and *S. scrofa* (82.8 °; Ekdale, 2009), and the angle between the ASC and PSC is the greatest one (*D. ilicis*: 95 °; *S. scrofa*: 96.0 °; Ekdale, 2009). The angle between the PSC and the LSC is slightly smaller in *D. ilicis* (81 °) than in *S. scrofa* (87.9 °; Ekdale, 2009). While the basic pattern of relative lengths and angles between the planes of the semicircular canals is similar in *D. ilicis* and *S. scrofa*, both taxa differ markedly in the shape of their semicircular canals. The ASC of *D. ilicis* is more dorsally extensive than is the posterior one, whereas in *S. scrofa*, both canals show similar dorsal extension. The semicircular canals of *D. ilicis* are more undulated than those of *S. scrofa*, which are almost each arranged in a single plane. The ampullae of *D. ilicis* are moderately inflated and more elongated compared with the rounded teardrop-shaped ampullae of *S. scrofa* (Ekdale, 2009; fig. 5.26). In *S. scrofa*, the posterior ampulla is located slightly ventral to the horizontal plane defined by the LSC (Fig. 2d vs. n), whereas in *D. ilicis*, the posterior and lateral ampullae attach to the vestibule in the same horizontal plane. In *S. scrofa*, the posterior limb of the LSC opens directly into the vestibule, dorsal to the posterior ampulla, without forming a secondary common crus.

Comparative functional study of the bony labyrinth of *Diacodexis* and the living tragulid *Moschiola*

Locomotor agility

As noted above, we ask here if the living tragulid *M. meminna* and extinct *Diacodexis*, which have similar limb proportions, also share similar locomotor agility signal in the semicircular canals. Agility scores assigned by Spoor et al. (2007) are integer values ranging from 1 to 6, with 1 corresponding to the less agile mammals (e.g. sloths) and 6 to the most agile ones (e.g. squirrel). Depending on the body mass estimates used, the coefficient of agility of *Diacodexis* ranges between 3.48 and 3.80, which corresponds to a medium slow or 'average' agility for mammals according to Spoor et al. (2007). Such values are found in terrestrial, cursorial, scansorial and semi-aquatic taxa. According to Spoor et al. (2007), *Diacodexis* would have been less agile than the antelope *Gazella* (agility score = 4). However, if we consider the 'average semicircular radius (SCR) mammal predictions' scores derived from Silcox et al. (2009) equa-

tion, living artiodactyls range between 2.4 (*S. scrofa*) and 3.4 (*Gazella bennetti*). Therefore, the SCR predictions of *Diacodexis* and *Moschiola* are greater than the SCR predictions for *Gazella*, when the theoretical equation for all mammals is used. It is also noteworthy that the SCR prediction for the extant rabbit *Oryctolagus* (SCR prediction score = 3.8) is similar to that estimated for *Diacodexis* using the smallest body mass. These results are congruent with the functional studies of *Diacodexis* based on postcranial remains, hypothesizing that it was a nimble, fast running to jumping animal (Rose, 1982, 2006).

Hearing capabilities

Based on the postulate that the sensitivity to low frequencies is located within the basal turn of the cochlea and high-frequency sensitivity is located at the apex (von Bekesy, 1960), West (1985) and Ketten et al. (1992) proposed that the shape of the cochlea was correlated with frequency sensitivity. Low-frequency hearing in a mammal correlates with a tightly coiled cochlea and/or high number of turns (e.g. in primates; Coleman & Colbert, 2010; Coleman et al. 2010). By contrast, mammals displaying a loosely coiled cochlea with a small number of turns are expected to be high-frequency specialists, such as odontocetes (Ketten et al. 1992). The relatively weak coiling of the cochlear canal of *Diacodexis* and *Moschiola* suggests rather high-frequency hearing capabilities for these taxa. The cochlear canals of both *Diacodexis* and *Moschiola* have a secondary bony lamina for the basilar membrane. The presence of this structure would suggest a narrow basiliar membrane, which is in turn correlated to rather limited low-frequency hearing capabilities (Fleischer, 1973; Ketten et al. 1992) and is congruent with the small number of coils.

The radii ratio (quotient between the radius of the basal turn and the radius of the apical turn of the cochlea) was demonstrated to be correlated with low-frequency hearing capabilities in a limited sample of mammals (Manoussaki et al. 2008). A large radii ratio is hypothesized to be correlated with acute ability to hear low frequencies. The value of this ratio in *Diacodexis* is 2.76, which corresponds to a low-frequency limit estimate of 543 Hz (at 60 dB) calculated with the Manoussaki et al. (2008) equation. The value of this ratio in *Moschiola* equals 4.60, which corresponds to a low-frequency limit estimate of 186.0 Hz (at 60 dB) using the same equation. These values are higher than the low-frequency limit of *S. scrofa* (33 Hz at 60 dB; Heffner & Heffner, 1990), of the cow, *Bos taurus* (23 Hz at 60 dB; Manoussaki et al. 2008) and of the white-tailed deer, *Odocoileus virginianus* (115 Hz; Heffner & Heffner, 2010). *Diacodexis* falls in the range of high-frequency specialists sampled by Manoussaki et al. (2008), such as *Rattus* (low-frequency limit = 390–530 Hz). The estimated low-frequency limit of hearing of *M. meminna* is higher than that of *O. virginianus*, but much lower than that of *D. ilicis* and does not coincide with a high-frequency specialization. However, as highlighted by Manoussaki et al. (2008), one must remain cautious about hearing capabilities estimates based on cochlear shape, as the correlation is currently based on a small sample (13 terrestrial and marine mammal species). Furthermore, some specialist mammals such as mole rats, some bats or the harbor porpoise do not fit the generalist correlation.

Diacodexis bony labyrinth – comparisons to other therian taxa

Basal phylogenetic relationships among artiodactyls remain a current topic of investigation. However, recent studies showed that stem taxa to extant artiodactyl groups are to be found in the paraphyletic assemblage of dichobunoid artiodactyls to which *Diacodexis* belongs (e.g. Geisler et al. 2007; Geisler & Theodor, 2009; Spaulding et al. 2009). While being the earliest representatives of Artiodactyla, *Diacodexis* species appear either as the first branch at the base of the Artiodactyla (e.g. Geisler et al. 2007; Geisler & Theodor, 2009), or more highly nested in the artiodactyl tree and closely related to cetaceans (Spaulding et al. 2009; Orliac & Ducrocq, 2011).

Morphology of the cochlear canal

The cochlear canal has at least one complete 360 ° turn in living therian mammals (Gray, 1907, 1908; Rowe, 1988), and a low value of cochlear coiling is hypothesized to be primitive for Eutheria, reaching 735 ° in the hypothetical common ancestor of placental mammals (Ekdale, 2009). The cochlear canal of *Diacodexis* completes two full whorls (720 °), a value smaller than that observed in extant *Sus* and *Moschiola* (Table 2). Based on the morphology of the bony labyrinth of *S. scrofa* (living suid), *Bathygenys reevesi* (extinct merycoidodontid, Eocene), *Tursiops truncatus* (living cetacean) and a fossil Balaenopteridae (extinct cetacean, age not specified), Ekdale (2009) reconstructed the ancestral morphology of the cochlea for the common ancestor of Artiodactyla. Ekdale (2009) estimated an ancestral cochlear coiling for artiodactyls of 845.8 ° (2.35 turns), a value less than that of living terrestrial members of the group. The low value of cochlear coiling of Eocene fossil artiodactyls described so far, *B. reevesi* (665 °; Ekdale, 2009) and *D. ilicis* (720 °), is congruent with the hypothesis that the earliest artiodactyls had relatively limited cochlear coiling.

In *Diacodexis*, the basal turn of the cochlea forms an acute angle with the plane of the lateral canal (12 °), and the vestibular and cochlear fenestrae are almost parallel to the LSC plane. This condition differs greatly from that of extant artiodactyls, which display a more opened angle (Table 2); a morphology similar to that of extant artiodactyls is also observed in the Oligocene merycoid-

odontid *Bathygenys* (26 °; Ekdale, 2009). Like living artiodactyls, most modern therian mammals, especially Ferungulata, display a widely open angle (e.g. *Felis*: 45.8 °; *Canis*: 20.8 °; *Equus*: 37.9 °; Ekdale, 2009). However, a small angle was observed in the Cretaceous eutherian mammals *Kulbeckia*, *Ukhaatherium* and *Zalambdalestes* (respectively, 12.1 °, 6.63 ° and 13.5 °; Ekdale, 2009, fig. 4.5, 2011), and the polarity of this character remains poorly understood in the absence of more specimens of Paleogene artiodactylans.

The basal turn of the cochlear canal of *Diacodexis* shows a clear lamina secundaria. Among Artiodactyla, a lamina secundaria is present in extant and extinct cetaceans (Ketten et al. 1992; Spoor et al. 2002; Ekdale, 2009) and described here in the tragulid ruminant *M. meminna*, but is absent in the suid *S. scrofa* (Ekdale, 2009). Its presence could not be assessed on the CT reconstruction of *Bathygenys* (Ekdale, 2009). Outside Artiodactyla, this structure is observed in most therian mammals (Meng & Fox, 1995; Ekdale, 2009).

Macrini et al. (2010) observed that the inner ear of the South American native ungulate *Notostylops* (Notoungulata, Eocene) differed from other eutherians in the extension of the cochlear aqueduct posterior to the plane of the PSC. The location and orientation of the cochlear aqueduct in artiodactyls is similar to that of *Notostylops*: it ascends posteriorly and forms a right angle with the plane of the PSC in dorsal view. A similar orientation exists in the perissodactyl *Equus caballus* (Ekdale, 2009, fig. 5.32). It would be important to assess the polarity of this character within 'ungulates'. *Diacodexis*, however, differs from other 'ungulates' studied to date in the relatively short length of its cochlear canal.

The fenestra cochleae of *Diacodexis* are directed laterally relative to the PSC plane. This orientation is also observed in *S. scrofa* and *M. meminna*, as well as in *E. caballus* (Ekdale, 2009; fig. 5.32). However, the fenestra cochleae extend posterior to the plane of the PSC in *Diacodexis*, a relationship that does not occur in *Sus* and *Moschiola*. A similar extension of the fenestra cochleae posterior to the PCS plane occurs in the Eocene archeocete cetaceans *Ichtyolestes* (pakicetid) and *Indocetus* (protocetid), as illustrated by Spoor et al. (2002). In the living dolphin *Tursiops*, the fenestra cochleae are located completely posterior to the PSC plane, while in balaenopterid cetaceans the fenestra cochleae have a posteriorly directed opening (Ekdale, 2009; fig. 5.28). A posterior location of the fenestra cochleae also occurs in some Cretaceous zhelestids and stem placentals: *Kulbeckia*, *Ukhaatherium*, *Zalambdalestes* (Ekdale, 2009; fig. 5.6; Ekdale & Rowe, 2011).

Semicircular canals

As described above, the secondary common crus corresponds to a fusion of the lumen of the bony channels of the PSC and LSC. This structure has been widely observed in a range of Cretaceous therians (Ekdale et al. 2004; Ekdale, 2009; Ekdale & Rowe, 2011) and in Cenozoic metatherians (Sánchez-Villagra et al. 2007; Schmelzle et al. 2007; Ekdale, 2009). It is present in extinct primates (Lebrun et al. 2010), extinct afrotherians (Benoit et al. in press) and extinct 'ungulates' (Russell, 1964), as well as in some extant ferungulate mammals such as Canidae and Orycteropodidae (Ekdale, 2009).

In his reconstruction of the bony labyrinth of the hypothetical common ancestor of Artiodactyla, Ekdale (2009) predicted that the common crus was absent and that the LSC opened into the vestibule directly at a superior position compared with the PSC. However, our work shows that a secondary common crus is present in the earliest artiodactyl *D. ilicis* and it is also present in the Eocene archaeocetes *Ichtyolestes pinfordi* and *Indocetus ramani*, as figured by Spoor et al. (2002, fig. 1). In *Ic. pinfordi*, the common crus is slender and shows the same morphology as in *D. ilicis*. In *Ic. pinfordi* and *D. ilicis*, the lateral canal enters the vestibule in a low position when compared with *Bathygenys* (Ekdale, 2009; fig. 5.24), *Moschiola* and *S. scrofa*, (i.e. at the level of the posterior ampulla). A secondary common crus occurs in all dichobunoid taxa investigated so far (e.g. *Homacodon*, *Dichobune*, *Cebochoerus*, *Gobiohyus*, *Helohyus*; Orliac & O'Leary, 2011), and we predict that the secondary common crus will optimize as present in revised phylogenetic studies reconstructing the hypothetical common ancestor of Artiodactyla once data on inner ear morphology are directly incorporated into a phylogenetic analysis. We also predict that this condition is later lost in certain artiodactyls, as has been observed independently in several other therian clades (e.g. Meng & Fox, 1995; Ruf et al. 2009; Ekdale & Rowe, 2011).

Conclusion

The bony labyrinth of *Diacodexis* differs greatly from that of modern artiodactyls previously described. *Diacodexis* shares with basal eutherian mammals the presence of a secondary common crus, a dorsal extension of the ASC that is more pronounced than that of the PSC, and a small angle between the basal turn of the cochlea and the LSC. These new data need to be incorporated into a large-scale phylogenetic analysis to determine if these characters were also present in the hypothetical common ancestor of Artiodactyla; we predict that many of them will be reconstructed in a revised concept of this ancestor.

Diacodexis has no living analog among artiodactyls in terms of size, but its overall body proportions, especially the hindlimbs, strongly resemble those of small tragulid ruminants. Comparison of the bony labyrinth of *Diacodexis* to that of the tragulid *M. meminna* (the Indian mouse deer) reveals great morphological differences in cochlear shape and semicircular canal disposition. The shape of the cochlea suggests that *Diacodexis* was a high-frequency hearing spe-

cialist, with a high low-frequency hearing limit (543 Hz at 60 dB). By comparison, the estimated low-frequency limit of one of the smallest living artiodactyl, *M. meminna*, is much lower (186.0 Hz at 60 dB). The limit of low-frequency hearing ability in *Diacodexis* is high, which is congruent with the hypotheses that: high-frequency hearing is present in many Late Mesozoic and Early Tertiary mammals that have been assessed for this; and low-frequency hearing abilities have appeared several times in different mammalian groups (Meng & Fox, 1995; Nummela & Sánchez-Villagra, 2006). The presence of long semicircular canals in *Diacodexis* (also in the living tragulid *Moschiola*) is congruent with the postcranial functional analysis that this extinct taxon was a nimble, fast running to jumping animal.

Acknowledgements

We are grateful to R. O'Leary (AMNH), J. Meng (AMNH), S. Jiquel (UM2) and B. Marandat (UM2) for access to the collections, and to J. Thostenson (AMNH), M. Hill (AMNH) and A.-L. Charruault (UM2) for assistance acquiring CT scans. We are grateful to P.-O. Antoine for constructive comments on earlier versions of the manuscript. Many thanks to the two reviewers, M. Silcox and T. Macrini, for their thorough review of the manuscript. This work has been possible thanks to the high-resolution CT scanner facility of the AMNH funded by the NSF MR1–R2 0959384 to N. Landman, D. Ebel and D. Frost, and to the Montpellier Rio Imaging platform (Montpellier, France). This is ISE-M publication 2012-117. This research was supported by the ANR funding project Palasiafrica, headed by L. Marivaux.

Authors' contribution

M. J. Orliac contributed the research design, acquisition of data, data analysis and interpretation, writing of the manuscript; J. Benoit and M. A. O'Leary contributed to the data analysis and interpretation, and to the critical revision of the manuscript.

References

Bajpai S, Kapur VV, Das DP, et al. (2005) Early Eocene land mammals from Vastan Lignite Mine, District Surat (Gujarat), western India. *J Palaeontol Soc India* **50**, 101–113.

Bajpai S, Thewissen JGM, Sahni A (2009) The origin and early evolution of whales: macroevolution documented on the Indian Subcontinent. *J Biosci* **34**, 673–686.

von Bekesy G (1960) *Experiments in Hearing*. New York: McGraw-Hill.

Benoit J, Orliac MJ, Tabuce R (in press) The petrosal of the earliest elephant shrew *Chambius* (Macroscelidea, Afrotheria) from the late early Eocene locality of Chambi (Tunisia) and the evolution of the middle and inner ear of elephant-shrews. *J Syst Paleontol*, in press.

Coleman MN, Colbert MW (2010) Correlations between auditory structures and hearing in non-human primates. *J Morphol* **271**, 511–532.

Coleman MN, Kay RF, Colbert MW (2010) Auditory morphology sensitivity in fossil new world monkeys. *Anat Rec* **293**, 1711–1721.

Coombs MC, Coombs WP (1982) Anatomy of the ear region of four Eocene Artiodactyls, *Gobiohyus*, ?*Helohyus*, *Diacodexis* and *Homacodon*. *J Vertebr Paleontol* **2**, 219–236.

Damuth J (1990) Problems in estimating body masses of archaic ungulates using dental measurements. In: *Body Size in Mammalian Paleobiology*. (eds Damuth J, MacFadden BJ), pp. 229–253. Cambridge: Cambridge University Press.

Ekdale EG (2009) Variation within the bony labyrinth of mammals. PhD dissertation. Austin, TX: The University of Texas, 456 pp.

Ekdale EG, Rowe T (2011) Morphology and variation within the bony labyrinth of zhelestids (Mammalia, Eutheria) and other therian mammals. *J Vertebr Paleontol* **31**, 658–675.

Ekdale EG, Archibald JD, Averianov AO (2004) Petrosal bones of placental mammals from the Late Cretaceous Uzbekistan. *Acta Palaeontol Pol* **49**, 161–176.

Fleischer G (1973) Studien am Skelett des Gehörorgans der Säugetiere, einschließlich des Menschen. *Säugetierkd Mitt* **21**, 131–239.

Geisler JGM, Theodor JM (2009) *Hippopotamus* and whale phylogeny. *Nature* **458**, 1190–1194.

Geisler JH, Theodor JM, Uhen MD, et al. (2007) Phylogenetic relationships of cetaceans to terrestrial artiodactyls. In: *The Evolution of Artiodactyla* (eds Prothero DR, Foss S), pp. 19–31. Baltimore: John Hopkins University Press.

Gingerich PD (1989) New earliest Wasatchian mammalian fauna from Eocene of northwestern Wyoming, composition and diversity in a rarely sampled high-floodplain assemblage. *Univ Mich Pap Paleontol* **28**, 1–97.

Godinot M (1981) Les mammifères de Rians (Eocène inférieur, Provence). *Palaeovertebrata* **10**, 43–126.

Gray AA (1907) *The Labyrinth of Animals: Including Mammals, Birds, Reptiles and Amphibians*, Vol. 1. London: J & A Churchill.

Gray AA (1908) *The Labyrinth of Animals: Including Mammals, Birds, Reptiles and Amphibians*, Vol. 2. London: J & A Churchill.

Guthrie DA (1971) The mammalian fauna of the *Lost Cabin* Member, Wind River Formation (lower Eocene) of Wyoming. *Ann Carnegie Mus* **43**, 47–113.

Heffner SR, Heffner HE (1990) Hearing in domestic pigs (*Sus scrofa*) and goats (*Capra hircus*). *Hear Res* **48**, 231–240.

Heffner H, Heffner HE (2010) The behavioral audiogram of whitetail deer (*Odocoileus virginianus*). *J Acoust Soc Am* **127**, 111–114.

Janis C (1990) Correlation of cranial and dental variables with body size in ungulates and macropodoids. In: *Body Size in Mammalian Paleobiology*. (eds Damuth J, MacFadden BJ), pp. 255–299. Cambridge: Cambridge University Press.

Ketten DR (1992) The Cetacean ear: form, frequency, and evolution. In: *Marine Mammal Sensory Systems*. (eds Thomas J, Kastelein RA, Supin AY), pp. 53–75. New York: Plenum Press.

Kumar K, Jolly A (1986) Earliest artiodactyl (*Diacodexis*, Dichobunidae: Mammalia) from the Eocene of Kalakot, northwestern Himalaya, India. *Bull Indian Soc Geoscient* **2**, 20–30.

Kumar K, Rose KD, Rana RS, et al. (2010) Early Eocene artiodactyls (Mammalia) from Western India. *J Vert Paleont* **30**, 1245–1274.

Lebrun R, De León MP, Tafforeau P, et al. (2010) Deep evolutionary roots of strepsirrhine primate labyrinthine morphology. *J Anat* **216**, 368–380.

Lovel JM, Harper GM (2007) The morphology of the inner ear from the domestic pig (*Sus scrofa*). *J Microsc* **228**, 345–357.

Luo Z, Gingerich PD (1999) Terrestrial Mesonychia to aquatic Cetacea: transformation of the basicranium and evolution of hearing in whales. *Univ Mich Pap Paleontol* **31**, 1–98.

Macrini TE, Flynn JJ, Croft DA, et al. (2010) Inner ear of a notoungulate placental mammal: anatomical description and examination of potentially phylogenetically informative characters. *J Anat* **216**, 600–610.

Manoussaki D, Chadwick RS, Ketten DR, et al. (2008) The influence of cochlear shape on low-frequency hearing. *Proc Natl Acad Sci USA* **105**, 6162–6166.

Martinez JN, Sudre J (1995) The astragalus of Paleogene artiodactyls, comparative morphology, variability and prediction of body mass. *Lethaia* **28**, 187–209.

Mendoza M, Janis CM, Palmqvist P (2006) Estimating the body mass of extinct ungulates: a study on the use of multiple regression. *J Zool* **270**, 90–101.

Meng J, Fox RC (1995) Osseous inner ear structures and hearing in early marsupials and placentals. *Zool J Linn Soc* **115**, 47–71.

Nummela S, Sánchez-Villagra MR (2006) Scaling of the marsupial middle ear and its functional significance. *J Zool* **270**, 256–267.

Orliac MJ, Ducrocq S (2011) Eocene raoellids (Mammalia, Cetartiodactyla) outside the Indian Subcontinent, palaeogeographical implications. *Geol Mag* **149**, 80–92.

Orliac MJ, Gilissen E (2012) Virtual endocranial cast of earliest Eocene *Diacodexis* (Artiodactyla, Mammalia) and morphological diversity of early artiodactyl brains. *Proc R Soc B* **279**, 3670–3677. doi: 10.1098/rspb.2012.1156.

Orliac MJ, O'Leary MA (2011) Endocranial structures of *Diacodexis* (Mammalia, Artiodatyla). *J Vertebr Paleontol* **31**(Abstract of the SVP meeting suppl.), 169.

Rose KD (1982) Skeleton of *Diacodexis*, oldest known artiodactyl. *Science* **216**, 621–623.

Rose KD (2006) *The Beginning of the Age of Mammals*. Baltimore: The John Hopkins University Press.

Rose KD, Chew AE, Dunn RH, et al. (2012) Earliest Eocene mammalian fauna from the Paleocene-Eocene thermal maximum at Sand Creek Divide, Southern Big Horn Basin, Wyoming. *Univ Mich Pap Paleontol* **36**, 1–122.

Rowe T (1988) Definition, diagnosis and origin of mammalia. *J Vertebr Paleontol* **8**, 241–264.

Ruf I, Luo Z–X, Wible JR, et al. (2009) Petrosal anatomy and inner ear structures of the Late Jurassic *Henkelotherium* (Mammalia, Cladotheria, Dryolestoidea): insight into the early evolution of the ear region in cladotherian mammals. *J Anat* **214**, 679–693.

Russell DE (1964) Les mammifères paléocènes d'Europe. *Mem Mus Natl Hist Nat (Ser C)* **8**, 1–324.

Sánchez-Villagra MR, Ladevèze S, Horovitz I, et al. (2007) Exceptionally preserved North American Paleogene metatherians: adaptations and discovery of a major gap in the opossum fossil record. *Biol Lett* **3**, 318–322.

Schmelzle T, Sanchez-Villagra MR, Maier W (2007) Vestibular labyrinth diversity in diprotodontian marsupial mammals. *Mammal Study* **32**, 83–97.

Silcox MT, Bloch JI, Boyer DM, et al. (2009) Semicircular canal system in early primates. *J Hum Evol* **56**, 315–327.

Smith R, Smith T, Sudre J (1996) *Diacodexis gigasei* n. sp., le plus ancient Artiodactyle (Mammalia) Belge, proche de la limite Paléocène-Eocène. *Bull Inst R Sci Nat Belg* **66**, 177–186.

Spaulding M, O'Leary MA, Gatesy J (2009) Relationships of Cetacea (Artiodactyla) among mammals, increased taxon sampling alters interpretations of key fossils and character evolution. *PLoS ONE* **4**, 1–14.

Spoor F, Zonneveld F (1998) Comparative review of the human bony labyrinth. *Yearb Phys Anthropol* **41**, 211–251.

Spoor F, Bajpal S, Hussaim ST, et al. (2002) Vestibular evidence for the evolution of aquatic behaviour in early cetaceans. *Nature* **417**, 163–166.

Spoor F, Garland T, Krovitz G, et al. (2007) The primate semicircular canal system and locomotion. *Proc Natl Acad Sci USA* **104**, 10 808–10 812.

Sudre J, Russell DE, Louis P, et al. (1983) Les artiodactyles de 1'Eocène inférieur d'Europe. *Bull Mus Natl Hist Nat, (Ser 4, sec C)* **5**, 281–365.

Thewissen JGM, Hussain ST (1990) Postcranial osteology of the most primitive artiodactyl *Diacodexis pakistanensis* (Dichobunidae). *Anat Histol Embryol* **19**, 37–48.

Thewissen JGM, Russell DE, Gingerich PD, et al. (1983) A new dichobunid artiodactyl (Mammalia) from the Eocene of northwest Pakistan. *Proc K Ned Akad Wet* **86**, 153–180.

Thewissen JGM, Cooper LN, George JC, et al. (2009) From land to water: the origin of whales, dolphins, and porpoises. *Evol Educ Outreach* **2**, 272–288.

West CD (1985) The relationship of the spiral turns of the cochlea and the length of the basilar membrane to the range of audible frequencies in ground dwelling mammals. *J Acoust Soc Am* **77**, 1091–1101.

Yang A, Hullar TE (2007) Relationship of semicircular canal size to vestibular-nerve afferent sensitivity in mammals. *J Neurophysiol* **98**, 3197–3205.